Conformation and Dynamics of Poly(oxyethylene) in Benzene Solution: Solvent Effect from Molecular Dynamics Simulation

Kenzabu Tasaki[†]

Department of Chemistry, Washington University, Campus Box 1134, St. Louis, Missouri 63130

Received February 21, 1996; Revised Manuscript Received October 15, 1996[⊗]

ABSTRACT: The detailed analysis of the conformation and the dynamics of poly(oxyethylene) (POE) in benzene solution is presented in order to examine the solvent effect relative to a POE aqueous solution. The analysis is based on a 5 ns molecular dynamics simulation of a POE chain with 15 repeating units in a solution of 191 benzene molecules. The results are compared to the previous simulation of the same POE chain in aqueous solution. The helical conformation taken from the simulation in an aqueous solution transformed to a random coil in 0.5 ns in a benzene solution. Further, much faster conformational transition rates around the internal bonds have been found in a benzene solution than in an aqueous solution, indicating a significantly smaller solvent damping effect on the POE chain in benzene solution. The C−C−O pairwise conformational populations are also compared with those obtained from the recent POE melt simulation in light of the POE chain dimension in different states. The chain conformation, the conformational populations, and the relaxation time for the C−H vector reorientation are all in good accord with the experiments.

Introduction

Poly(oxyethylene) (POE) is of significant industrial, in particular biomedical,[1] importance due in part to its unique solubility in both water and a wide range of organic solvents. The solution properties of POE are known to be very sensitive to the solvent.[2] In fact, POE exhibits a number of interesting characteristics in aqueous solutions such as a high solution viscosity, a phase separation at a cloud point, a psuedoplastic rheological behavior, and a helical conformation, many of which are not found in organic solutions.[2] Due to lack of sufficient experimental data, however, thorough comparison of POE characteristics between aqueous and organic solutions is often difficult. It is thus not very clear what the fundamental difference is in the solution properties of POE between aqueous and organic solutions; therefore, it remains equivocal what the role of water is in the conformation and the dynamics of POE in aqueous solution. The difference in the effect of the solvent, the relative solvent effect, on the POE properties between aqueous and organic systems is our primary interest in this study.

This report is one of a series to investigate the solution properties of POE in a wide variety of solvents by an atomistic computer simulation in order to gain insight into POE conformational and dynamical characteristics in different solvents. The conformation and the dynamics of POE in different environments play an important role in a variety of properties. A number of computer simulations have been successfully applied to polymers in glassy states, melts, and crystals.[3] On the other hand, computer modeling of synthetic polymer/solvent systems is less explored, compared to amorphous polymers.[4] Previously, we have performed a molecular dynamics (MD) simulation of POE in a dilute aqueous solution.[5] We found that water had a strong effect through its hydrogen bonds on characteristics of POE in aqueous solution. POE is a unique polymer in that it has both hydrophilic and hydrophobic groups along the backbone chain. The interactions of both groups with water have been studied in detail.[5] It is of considerable interest to investigate the interactions with a hydrophobic solvent.

In this article, we report an MD simulation of POE in a dilute benzene solution. We first characterize the conformation and the dynamics of POE in detail and then examine the difference in the conformational and dynamic properties of POE in going from a highly polar protic solvent, water, to a nonpolar organic solvent, benzene. We chose benzene as a solvent since benzene is a nonpolar, aprotic solvent with no hydrophilic group. Thus such effects as the hydrogen bond and the high polarization effect of water can be eliminated from POE's characteristics in benzene solution, while the hydrophobic effect of benzene still remains. This makes it possible to examine the role of the hydrogen bond and the polarization of water on the conformation and the dynamics of POE in aqueous solution. Furthermore, a number of experimental data of POE in benzene solutions[2a−g] are available for calibration of the simulation. Nonetheless, no quantitative analysis of the POE conformation in benzene solution has been presented except for the rotational isomeric state analysis based on its dipole moment.[6]

We observed from the previous simulation that POE assumed a helical conformation in an aqueous solution which remained throughout the 2 ns of simulation.[5] The helix structure was ascribed to its fitness to the water structure and the strong hydration of the helix. However, the helical conformation might have been an artifact due to the insufficient simulation time. Examination of the POE conformation using the same simulation protocol in benzene may help verify the POE helix as a result of the solvation. It is known that POE adopts a random coil conformation in benzene.[2a,d] POE has also been reported to have more chain flexibility in benzene solution than in aqueous solution.[2a−g] Our interests in the relative solvent effect here include the chain dimension and conformation, the local conformation and chain dynamics, and the high field shift of the methylene ^{1}H NMR chemical shift observed in benzene solution.[2b] Comparison of the results from POE simulations in an organic solvent with experiment has not been

[†] Current address: Mitsubishi Chemical America, Inc., 99 W Tasman Dr. Suite 200, San Jose, CA 95134.

[⊗] Abstract published in *Advance ACS Abstracts,* December 15, 1996.

S0024-9297(96)00278-1 CCC: $12.00

reported. Also, this is a part of our effort to develop (or calibrate) a force field to describe the conformational and dynamical behaviors of POE in various solvents. One of our future goals is to model POE in two-phase systems, e.g., a water−organic solvent system, of great scientific and industrial interest.

Recently, MD simulations of POE melts have been performed by Smith and cowokers.[7] It was found that in going from the unperturbed chains to the melts, the gauche$^{\pm}$−trans conformational population for the C−C−O bond pair increased, while the gauche$^{\pm}$−gauche$^{\mp}$ population decreased. They claimed that those population changes resulted from the intermolecular O···CH$_2$ interactions, giving rise to an extended POE chain in the melts. Small angle neutron scattering measurement has observed that the POE's molecular dimension in the melts is extended,[8] relative to the chain in Θ solutions.[9] Similar conformational changes have been also found for 1,2-dimethoxyethane (1,2-DME), a low molecular weight analogue of POE, in going from the gas phase to the liquid by MD simulations, which has been also attributed to the same intermolecular O···CH$_2$ interactions.[10] However, an NMR study has shown very similar vicinal coupling constants for 1,2-DME in both the liquid and dilute nonpolar solutions.[2j,11] This result implies little difference in the conformational populations of 1,2-DME between the liquid and the solutions with no appreciable intermolecular O···CH$_2$ interactions, which seems to contradict with Smith et al.'s finding.[7] We analyze the pairwise conformational populations of POE in a benzene solution to see whether they differ from those in the melts. Though it is believed that the conformation of POE in both organic solvents and the melts is a random coil,[2a] the difference in the conformation is not well understood in detail between these states.

A short MD simulation (120 ps) of POE in a benzene solution has been previously reported.[12] Here, we have performed a 5 ns MD simulation for a similar size POE chain in an attempt to examine how long is sufficient for an MD simulation of the current size of the POE chain used to allow the chain to reach its equilibrium. Time evolutions of the equilibrium characteristics are presented for this purpose. The force field used in our MD simulation was originally developed by Smith et al.[13] Due to the different potential energy function adopted in our simulation, the potential function commonly used in popular commercial software packages such as QUANTA[14] and SYBYL,[15] we start with the adjustment of Smith et al.'s parameters[13] to our potential energy function.

Potential Energy Function

The potential energy function used in our MD simulation was the same as that used in our previous simulations in aqueous solution:[5]

$$V = \sum k_r(r - r_0)^2 + \sum k_\theta(\theta - \theta_0)^2 + \sum k_\phi\{1 + \cos(n\phi - \delta)\} + \sum 4\epsilon_{ij}\{(\sigma_{ij}/r_{ij})^{12} - (\sigma_{ij}/r_{ij})^6\} + \sum (q_i q_j/r_{ij}) \quad (1)$$

which represents, in the order, the bond stretching, the bond angle bending, the torsion potential, the van der Waals interactions, and the electrostatic interactions, respectively. In the previous simulations, the atomic charges and the torsion potential were parametrized for the POE−aqueous system, while the rest of the parameters were taken from the force field developed by Smith et al.[13] Here, we adopted the potential energy parameters directly from Smith et al.'s force field[13] since they are more relevant for a POE−nonpolar solvent system.[16] The same values were used for the atomic charges (q_i), the stretching force constants (k_r), the bending force constants (k_θ), and the reference bond lengths (l_0) and angles (θ_0) except for the COC bond angle (θ_0^{COC}). Our previous ab initio study[17] has shown that the bond angle COC of 1,2-DME optimized by MP2 gradient calculations is about 3° smaller than that optimized at the Hartree−Fock level on which Smith et al.'s force field is based.[18] Thus, we used $\theta_0^{COC} = 108°$ to reproduce the MP2 bond angle. As for the other parameters, we made adjustment due to the different potential energy function used in our simulation. For example, Smith et al. used a Buckingham type potential for van der Waals interactions, $\sum A_{ij} \exp(-r_{ij}B_{ij}) - C_{ij}r_{ij}^{-6}$, and $\sum (k_\varphi/2)\{1 - \cos n(\varphi - \varphi_0)\}$ for the torsion potential.[13] In our potential, the Lennard-Jones parameters were determined so as to reproduce the potential well depths (ϵ_{ij}) and the van der Waals radii ($2^{1/6}\sigma_{ij}$) of the atomic pair interaction potentials used by Smith et al. The torsion terms were reparametrized on the basis of the gas-phase ab initio calculations of 1,2-DME.[17,18] Table 1 lists only the values of the parameters different from those developed by Smith et al.[13]

Table 1. Potential Energy Parameters

Nonbonded Interaction Parameters

	$4\epsilon_{ij}\{(\sigma_{ij}/r_{ij})^{12} - (\sigma_{ij}/r_{ij})^6\}$	
interacting pair	ϵ_{ij}, kcal mol^{-1}	σ_{ij}, Å
C···C	0.095	3.44
C···O	0.138	3.15
O···O	0.199	2.85
C···H	0.031	3.23
O···H	0.044	2.93
H···H	0.098	3.00

Torsion Parameters

	$k_\phi\{1 + \cos(n\phi - \delta)\}$		
torsion	k_ϕ, kcal mol^{-1}	δ, deg	n
CC−OC	−3.50	0.0	1
CC−OC	1.40	180.0	2
CC−OC	0.50	0.0	3
OC−CO	−1.35	180.0	2
OC−CO	0.60	0.0	3
HC−OC[a]	0.40	0.0	3

[a] Taken from ref 13.

Table 2 shows a comparison in the conformational energetics and the optimized geometries for 1,2-DME between ab initio and force field calculations. The results of the ab initio calculations were taken from Jaffe et al.'s results obtained at the MP2/D95+(2df,p) level,[18] and the force field calculations used the parameters listed in Table 1 and the rest of the parameters taken from ref 13. The results obtained from Smith et al.'s force field calculations[13] are also shown in the parentheses. The agreement of our force field results with the ab initio calculations is comparable to that of Smith et al.'s[13] except for the relative energies for $tG^{\pm}g^{\pm}$ and $g^{\pm}G^{\mp}g^{\pm}$. These conformers have relatively high energies, and the agreement for the lower-energy conformers is excellent. The optimized bond angles by the current potential energy parameters show a better agreement with the MP2 geometries of 1,2-DME[17] than those optimized by Smith et al.'s force field[13] based on the Hartree−Fock geometries.

Table 2. Comparison between MP2 Ab Initio and Force Field Calculations for 1,2-DME

Energetics and Torsion Angles

	ab initio[b]			force field[c]			
conformer[a]	E[d]	ϕ_{CO}[e]	ϕ_{CC}[f]	E[d]	ϕ_{CO}[e]		ϕ_{CC}[f]
tTt	0.0	180.0	180.0	0.00	180.0 (179.9)		180.0 (−179.9)
$tG^{\pm}t$	0.15	175.3	73.6	0.10 (0.14)	180.0 (−177.6)		74.8 (77.2)
$tG^{\pm}g^{\mp}$	0.23	179.1, −84.2	75.1	0.21 (0.19)	180.0 (−178.5), −65.3 (−79.9)		84.8 (85.1)
$tTg^{\pm}$	1.43	179.4, 78.7	175.1	1.43 (1.38)	180.0 (−179.1), 66.4 (85.0)		163.7 (175.2)
$tG^{\pm}g^{\pm}$	1.51	179.3, 68.0	61.7	2.02 (1.74)	180.0 (−178.3), 61.6 (86.0)		58.1 (73.4)
$g^{\pm}G^{\pm}g^{\pm}$	1.64	63.9	48.3	2.42 (3.19)	60.6 (82.3), 60.9 (82.3)		48.2 (64.4)
$g^{\pm}G^{\pm}g^{\mp}$	1.86	83.0, −81.3	73.4	2.79 (1.70)	68.9 (79.1), −73.6 (−81.4)		92.3 (77.2)
$g^{\pm}G^{\mp}g^{\pm}$	2.41	110.6, 110.2	−65.7	4.11 (2.07)	86.1 (106.5), 86.0 (106.5)		−144.5 (−74.9)
$g^{\pm}Tg^{\mp}$	3.08	86.8, −86.9	180.0	2.95 (2.64)	91.5 (86.2), −66.4 (−86.2)		159.0 (179.1)
$g^{\pm}Tg^{\pm}$	3.13	82.9, 82.8	180.0	3.76 (2.66)	89.5 (83.4), 92.0 (83.4)		178.8 (167.9)
tCt	8.9	180.0	0.0	8.43 (8.9)	180.0	0.0	
tTc	7.24			7.29 (6.71)	180.0	180.	
$tTt{-}tG^{\pm}t^{g}$	2.31	−178.6	120.0	2.45 (1.88)	180.0	120.0	
$tTt{-}tTg^{\pm}$[h]	2.04	178.2, 117.4	178.7	2.77 (1.97)	180.0, 120.0	180.0	

Optimized Geometry

	ab initio[i]				force field[c]			
	r_{CC}	r_{CO}	θ_{COC}	θ_{CCO}	r_{CC}	r_{CO}	θ_{COC}	θ_{CCO}
tTt	1.52	1.41	111.2	107.4	1.52	1.40	111.7	108.9
					(1.52)	(1.40)	(113.8)	(108.8)
$tG^{\pm}$t	1.51	1.41	111.2	108.9	1.52	1.40	111.8	109.1
					(1.52)	(1.40)	(113.9)	(108.6)
$tG^{\pm}g^{\mp}$	1.52	1.41	113.6	113.9	1.53	1.41	113.8	112.3
		1.42	111.2	109.9		1.40	111.6	109.6
$tTg^{\pm}$	1.52	1.42	112.9	112.4	1.53	1.41	113.9	112.0
		1.42	111.3	107.1		1.40	111.8	108.9
$tG^{\pm}g^{\pm}$					1.53	1.41	114.4	112.9
						1.40	111.9	109.1

[a] The lower case refers to the conformation around the C−O bond, the upper case denotes the conformation around the C−C bond, and *C* or *c* denotes the cis conformation where the oxygens are cis with respect to each other via the C−C bond or the methoxy carbon is cis with respect to the methylene carbon around the C−O bond, respectively. [b] Taken from ref 18. [c] Calculated by using the parameters listed in Table 1 and the rest of the parameters taken from ref 13. [d] The relative energy in kcal mol^{-1}. [e] The torsion angle around the C−O bond in degrees. [f] The torsion angle around the C−C bond in degrees. [g] The conformer at the rotational barrier in going from *tTt* to *tGt*. [h] The conformer at the rotational barrier in going from *tTt* to *tTg*. [i] Calculated at the MP2/6-311+G** level taken from ref 17. The numbers in parentheses are obtained from Smith et al.'s force field parameters.[13]

A number of potential energy functions have been proposed for a benzene molecule with different accuracy.[19] For the simplicity of the force field, we have adopted Jorgensen's OPLS parameters: no charge on each CH united atom.[20,21] The geometry of the benzene molecule was taken from the standard parameters used in conjunction with the OPLS parameters. Benzene molecules were treated as a rigid molecule with no internal degree of freedom.

MD Simulation Protocol

The detail of the MD simulation protocol was described elsewhere.[5] Here, we only describe the procedure relevant to the POE−benzene solution simulation. The system consisted of a POE chain with 15 repeating units, $C_{32}H_{66}O_{16}$, surrounded by 191 benzene molecules in a cubic primary box subject to periodic boundary conditions. The helical conformation obtained from the POE−aqueous solution simulation[5] was superimposed on the coordinates of a well-equilibrated cubic box of benzene molecules. Those benzene molecules which overlapped any of the POE atoms were eliminated from the system, and then the box length was set to 30.32 Å to yield the density of 0.881 g cm^{-3} for the POE−benzene solution at room temperature and at 1 atm. The concentration of this resulting solution was 0.058 M.

The system was first minimized to eliminate any van der Waals contacts between POE and benzene molecules through 100 steps of the steepest descent method. Equilibration was then performed for 100 ps during which atomic velocities were either scaled or assigned if the temperature deviated by ±5 K from 300 K. Subsequently, the simulation was continued for 5 ns for data collection. The temperature and the total energy were continuously monitored during the equilibration and thereafter and remained constant with small drifts after the first 50 ps of the equilibration until the end of the simulation. The simulation was performed on a Silicon Graphics Power Challenge and required 10 days of CPU time on one R8000 processor to complete the 5 ns simulation.

Benzene Liquid

A total of 216 benzene molecules were placed on lattice sites in a cubic box with 31.76 Å of the box length to yield the density of 0.874 g cm^{-3} at room temperature. The system was first heated to 500 K and then equilibrated for 20 ps, followed by cooling to 300 K and equilibrating for 20 ps. The simulation was continued for another 200 ps from which the structural and dynamic properties of benzene molecules were analyzed. The pair distribution function for the benzene carbon atom calculated from the dynamic trajectory was reasonably in good agreement with the X-ray measurement.[22] The self-diffusion coefficient of the center of mass of the benzene molecule, 2.13×10^{-5} cm^2 s^{-1}, calculated from its mean-square displacements also agrees well with the thermodynamic data, 2.2×10^{-5} cm^2 s^{-1}.[23]

Overall Conformation

Figure 1a illustrates the trajectory of the end-to-end distance (R) and the radius of gyration (S) of the POE

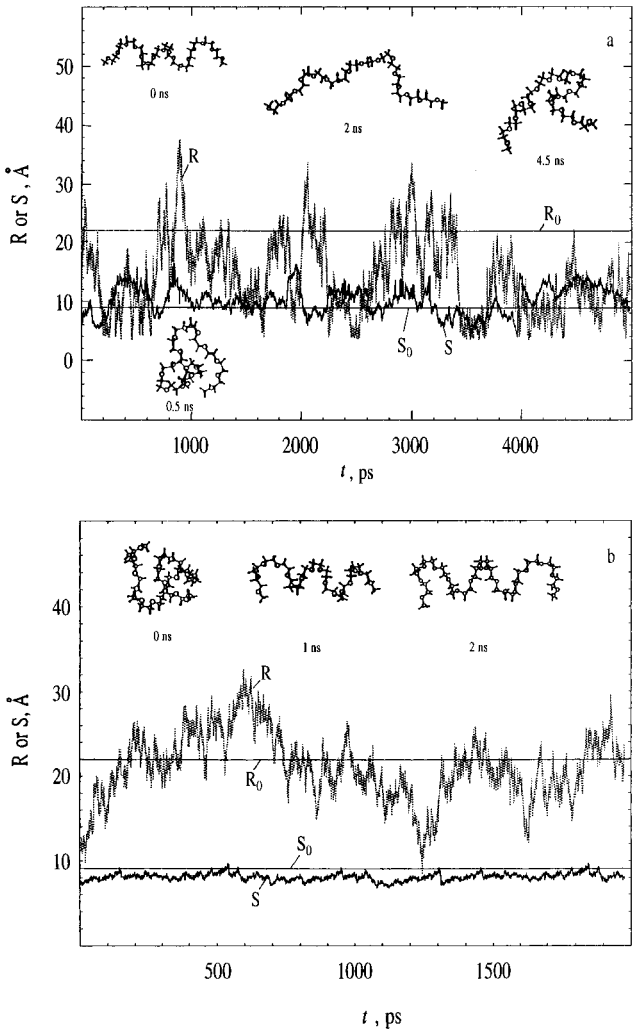

Figure 1. (a) Trajectories of the end-to-end distance (R) (a dotted line) and the radius of gyration (S) (a solid line) of the POE chain in a benzene solution and (b) those in an aqueous solution. Snapshots are shown at various stages of the simulation. The root-mean-square end-to-end distance (R_0) and the radius of gyration (S_0) for an unperturbed chain are indicated by a solid straight line.

chain in a benzene solution along with snapshots of the chain at various stages of the simulation. Also shown is the unperturbed root-mean-square end-to-end distance (R_0) calculated from the observed molecular dimension of POE in Θ solvents[9] for the current size of the chain. The root-mean-square radius of gyration for the unperturbed state, S_0, included in the figure was estimated with an assumption that the square radius of gyration at the unperturbed state is one-sixth of the unperturbed square end-to-end distance.

The helical conformation in the beginning of the simulation, taken from the previous simulation,[5] quickly broke down to a more disordered conformation by the first 0.5 ns. The POE chain stayed in a coiled conformation until the end of the simulation, in good agreement with the experiment,[2a,d] a sharp contrast to the ordered helix found throughout the POE-water simulation.[5]

There seem to be two types of fluctuations in the variations of R and S: the large "amplitudes" ranging from $R = 4$ Å to $R = 38$ Å and the small "fluctuations" associated with the amplitudes in a benzene solution. The root-mean-square distance ($\langle R^2 \rangle^{1/2}$) averaged over 5 ns is 15.66 ± 6.64 Å. The values of S vary less than

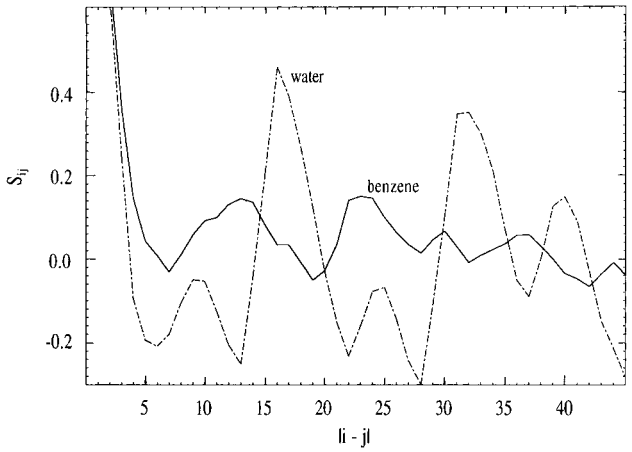

Figure 2. Bond direction correlation function S_{ij} between skeletal chords as a function of the index difference $|i - j|$. The results were averaged over 1000 trajectory frames. A few error bars are included based on the rms in the values of $\langle \cos^2 \theta \rangle$.

those of R: $\langle S^2 \rangle^{1/2} = 10.12 \pm 2.62$ Å. Similar behavior was observed by Tanaka and Mattice in their gas-phase simulation of a poly(vinyl chloride) chain.[24] The current size of the POE chain, 15 monomer units, is too short to reproduce the experimentally observed R_0 in a benzene solution.[25]

Similar plots for the POE aqueous solution are displayed in Figure 1b, taken from the previous simulation.[5] The amplitudes are about the same as those for the benzene solution, while the fluctuations are smaller. The POE chain stayed in a helix with the end-to-end distance between 8 and 32 Å. The value of $\langle R^2 \rangle^{1/2}$, 20.91 ± 3.97 Å, is larger than that for the benzene solution, while the value of $\langle S^2 \rangle^{1/2}$, 8.1 ± 0.4 Å, is coincidentally close to S_0. The fluctuations in R and S suggest a higher degree of freedom in the bond rotation along the chain in a benzene solution than that in an aqueous solution, consistent with the experiments.[2a-f]

In order to examine the difference in the chain behavior between both solutions in detail, we calculated the order parameter, $S = (3\langle \cos^2 \theta \rangle - 1)/2$.[26] S_{ij}, the bond orientational correlation, was obtained by taking the average over all the bond chord pairs in the backbone chain with given index difference $|i - j|$ and over 1000 frames of the trajectories. θ is the angle between two skeletal bond chords of the chain. Figure 2 shows a striking contrast in S_{ij} between the two solutions as a function of $|i - j|$. In a benzene solution, S_{ij} gradually decreases with increasing distance, and little directional correlation is shown at long distances, indicating a random coil-like behavior, while a large oscillatory correlation remains along the chain in an aqueous solution due to the helical conformation.

In the previous study,[5] we examined the structural fitness of the POE helix to the water structure by comparing the pair distribution function (PDF) for the POE oxygen atoms and that for bulk water oxygen atoms. We found an excellent agreement in peak position between the two PDF's. This agreement was interpreted as a manifestation of a good structural fit of the POE helix to the water hexagonal structure. Figure 3 displays the PDF for the oxygen atoms of the POE coil calculated from the current simulation in a benzene solution (a), along with the PDF's for the helical POE oxygen atoms in an aqueous solution (b) and for the bulk water oxygen atoms (c).[27] The first peak is split to two in the PDF a: one for the oxygens in a gauche

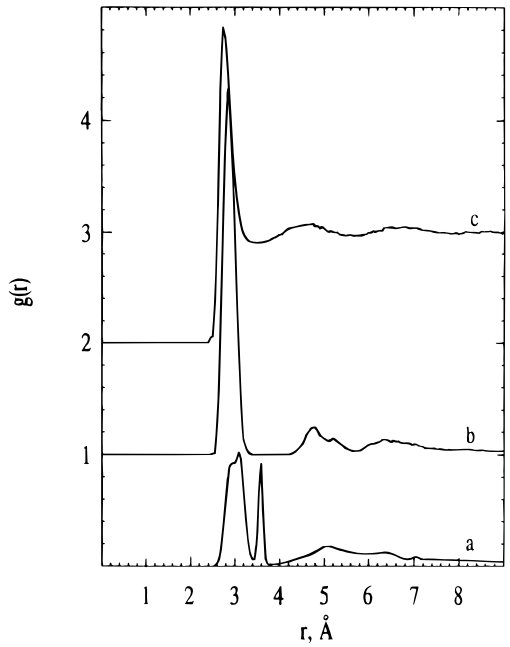

Figure 3. Pair distribution functions for the POE oxygen atoms (a) in a benzene solution, (b) in an aqueous solution, and (c) for the bulk water oxygen atoms. The results for (b) and (c) were taken from refs 5 and 27, respectively, and are shifted by 1 and 2 along the ordinate, respectively.

position around the C−C bond, ∼3 Å, and the other for those in a trans position, ∼3.6 Å. No trans conformation around the C−C bond was observed in an aqueous solution except for the terminal bonds (the PDF b). A somewhat broad peak of the PDF a around 3 Å results from a wide range in the values of the C−C torsion angles, e.g., $\langle\phi_{G\pm}\rangle_i$ (i = 2−14) = 68−95° (Δ = 27°), averaged over the simulation, compared to those, 54−73° (Δ = 19°), in an aqueous solution.[28] The larger values of $\langle\phi_{G\pm}\rangle_i$ also give rise to a shift in the first peak position from 2.9 Å in the aqueous solution to 3.2 Å in a benzene solution, which disagrees with the first peak at 2.8 Å for the bulk water oxygens, as do other peaks.

The second peak and its shoulder of the PDF b have been attributed to the $-[tG^{\pm}t]_i[tG^{\mp}t]_{i+1}-$ and the $-[tG^{\pm}t]_i$-$[tG^{\pm}t]_{i+1}-$ conformational sequences, respectively, in which the brackets [ ] denote an ethylene oxide (EO) unit.[5] Averaging over both conformational sequences as a result of a random coil led to the second peak around 5 Å in the PDF a. The disagreement in peak position between the PDF a and c implies an unfavorable random coil chain conformation in aqueous solution. Depner et al. also found no difference in the C−C bond conformational preference, the gauche or the trans, with respect to the interactions with benzene molecules.[12] Our observation including the above results for the chain conformation is consistent with various experimental studies reporting a significant change in going from aqueous solution to an organic solvent.[2a−g]

In order to compare the POE-solvent interactions between the two solutions, we calculated the total POE-solvent interaction energy which is a summation of interaction energies for all POE-solvent molecule pairs. The total POE-benzene molecule interaction energy averaged over 5 ns was −0.46 kcal mol^{-1}, while the averaged total POE-water molecule interaction energy was −96.52 kcal mol^{-1}, of which −97.75 kcal mol^{-1} was contributed from the electrostatic interactions. The positive van der Waals energy was due to the repulsive interactions associated with the water molecules confined inside the helix.

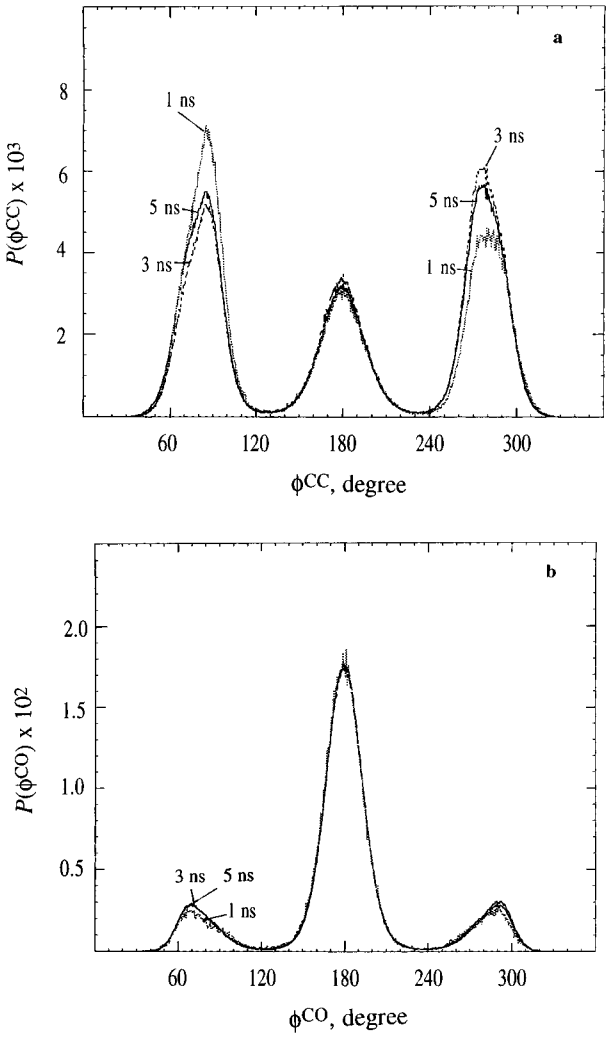

Figure 4. Torsion angle distributions (a) $P(\phi^{CC})$ around the C−C bond and (b) $P(\phi^{CO})$ around the C−O bond of POE, respectively, averaged over 1 ns (a dotted line), 3 ns (a broken line), and 5 ns (a solid line) in a benzene solution.

Local Conformation

A number of articles have been reported regarding the relationship between the simulation period and configurational equilibrium of condensed systems.[29] Due to a limited computer time, it is difficult to determine whether the system satisfies the ergodicity. Here, we only examine the time evolutions of local conformational characteristics of the POE chain in an attempt to obtain an "*equilibrium value*" in a sense that a further simulation would not yield a significantly different result. The gauche conformations around the C−C or C−O bonds of POE are mirror images to each other. Thus, the torsion angle distributions are a good measure for the conformational equilibrium of POE. Figure 4 illustrates the time evolution of the torsion angle distributions $P(\phi^{CC})$ and $P(\phi^{CO})$ around the C−C and the C−O bonds of POE in benzene, respectively, the mean values over the entire chain except for the terminal EO units. The distributions were averaged over 1, 3, and 5 ns. The distribution around the C−C bond does not become symmetric until 5 ns, while the C−O bond torsion angle distribution assumes a symmetric curve after 1 ns. The implication of the symmetric torsion angle distribution is an isomerization for both C−C and C−O bond rotations, as is required by their symmetric gauche rotamers $G^{\pm}/g^{\pm}$, and also a random coil for the chain

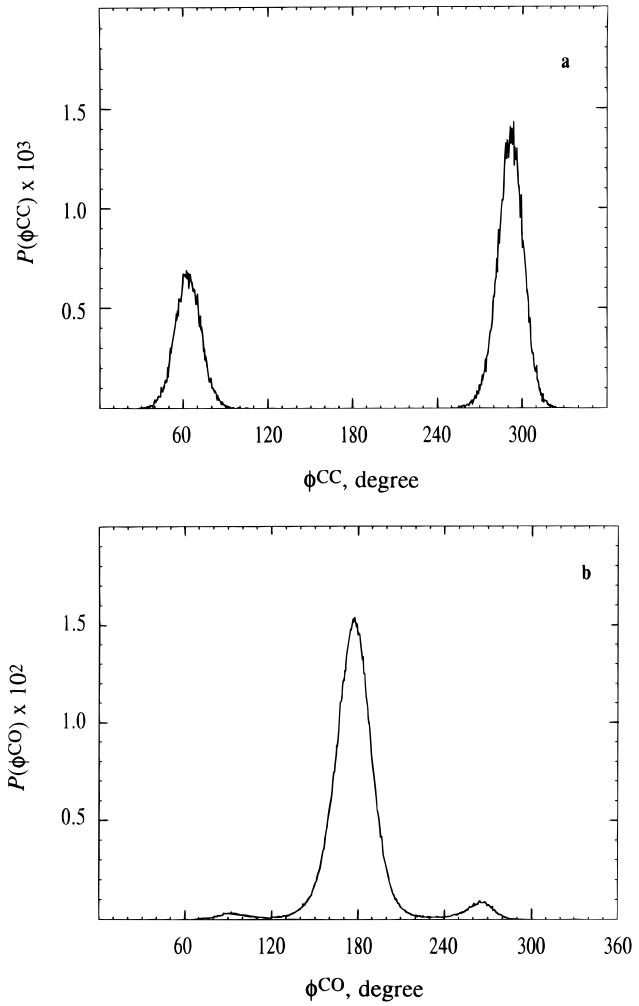

Figure 5. Torsion angle distributions (a) $P(\phi^{CC})$ around the C−C bond and (b) $P(\phi^{CO})$ around the C−O bond of POE, respectively, averaged over 2 ns in an aqueous solution. The figures were taken with permission from ref 5.

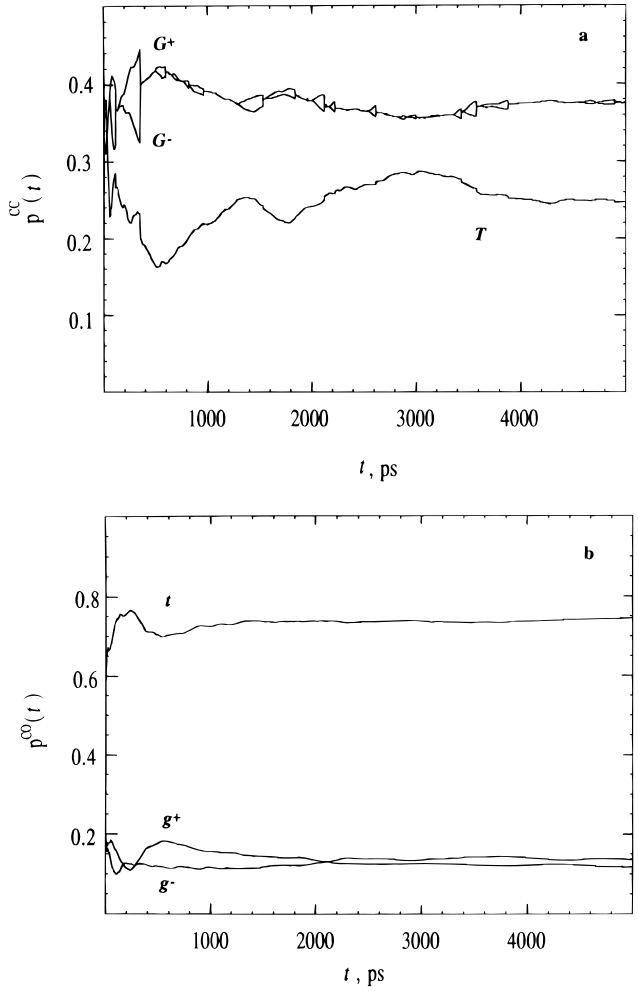

Figure 6. Time evolution of conformational populations $p^{CC}(t)$ and $p^{CO}(t)$ for the trans (T/t) and gauche ($G^{\pm}/g^{\pm}$) conformations around (a) the C−C bond and (b) the C−O bond of POE, respectively, in a benzene solution. See the text for the definition.

conformation, which is in good agreement with the experiments.[2a,d] Torsion angle distributions for individual bonds also showed similar characteristics. On the other hand, in an aqueous solution, the POE helix resulted in an asymmetric torsion angle distribution around the C−C bond, as is shown in Figure 5. The distribution profiles for the C−C and C−O bonds in an aqueous solution remained the same after 1 ns.

Figure 6 displays the conformational populations, $p^{CC}(t)$ and $p^{CO}(t)$, averaged over a given time period t. They are defined by $p_j^{CC(CO)}(t) = \sum n_j^{CC(CO)}(t)/N(t)$ where $n_j^{CC(CO)}(t)$ is the number of the cumulative time steps for conformation j around the C−C (C−O) bond averaged over the chain up to time t and $N(t)$ is the total number of time steps. The summation is over the total time frames up to t. $T(t)$, $G^+(g^+)$, and $G^-(g^-)$ are defined as the conformers with $120° \le \phi < 240°$, $0° \le \phi < 120°$, and $240° \le \phi < 360°$, respectively. $p^{CC}(t)$ evolves slowly with time, and it is only after around 4 ns that the average conformational populations become somewhat leveled. The conformational isomerism around the C−O bond, on the other hand, reaches its equilibrium more quickly by around 2 ns. Both observations are consistent with the time evolution of the torsion angle distributions. Further, many conformational transitions, approximately several hundreds, occurred around each C−C and C−O bond during the 5 ns simulation. Based on the above observations, the conformational characteristic of the POE chain seems to have reached at least its *quasi-equilibrium value* in 5 ns, if not completely the *equilibrium value*.

The gauche populations around the C−C and C−O bonds averaged over the chain except for the terminal bonds for 5 ns are $p_{G^+} = 0.37$, $p_{G^-} = 0.38$, $p_{g^+} = 0.12$, and $p_{g^-} = 0.12$, respectively. The estimated populations are close to those previously reported for POE which have been adjusted to reproduce the dipole moment of POE in benzene solution by the rotational isomeric state (RIS) model[6] ($p_{G^\pm} = 0.67$ and $p_{g^\pm} = 0.24$) and also similar to the populations determined in nonpolar solvents by NMR spectroscopy ($p_{G^\pm} = 0.66$ and $p_{g^\pm} = 0.24$).[2j] On the other hand, Depner and Schürmann's 120 ps simulation showed larger populations for $p_{G^\pm}$ (0.85) and $p_{g^\pm}$ (0.3).[12] It is not clear, however, in their simulation that the conformational populations reached the equilibrium values at 120 ps. In contrast, in an aqueous solution, we found that $p_{G^\pm} = 1.00$ and $p_{g^\pm} = 0.06$.[5] An NMR study has shown a significant solvation effect on the conformational energies for both C−C and C−O bonds of POE.[2j]

Additionally, we computed the pairwise conformational populations p^{CCO} for the C−C−O bond pair. From MD simulations of POE melts and unperturbed chains, Smith et al. have recently found an increase in the population of the $G^\pm t$ conformation ($p_{G^\pm t}^{CCO}$) and a decrease in the population of $G^\pm g^\mp$ ($p_{G^\pm g^\mp}^{CCO}$) in going

Table 3. Pairwise Conformational Populations for C−C−O Bond Pair[a]

system	$p_{G^{\pm}t}^{CCO}$	$p_{G^{\pm}g^{\mp}}^{CCO}$	p_{Tt}^{CCO}	$p_{Tg^{\pm}}^{CCO}$	$p_{G^{\pm}g^{\pm}}^{CCO}$
benzene solution	0.52	0.25	0.14	0.05	0.04
melt[b]	0.60	0.12			
unperturbed[b]	0.51	0.22			
aqueous solution[c]	0.85	0.01	0.04	0.01	0.09

[a] The results was averaged over all the internal bonds. [b] At 300 K taken from ref 7. [c] Taken from ref 5.

Table 4. Average Geometrical Parameters of POE in Benzene and Water Obtained from Simulations

Bond Lengths and Angles

solvent	r_{CC}[a]	r_{CO}[a]	θ_{CCO}[b]	θ_{COC}[b]
C_6H_6	1.52 ± 0.02	1.40 ± 0.02	109.8 ± 2.4	113.1 ± 2.3
H_2O	1.52 ± 0.02	1.41 ± 0.02	109.8 ± 2.2	112.2 ± 2.2

Torsion Angles

solvent	ϕ_T[c]	ϕ_{G^+}[d]	ϕ_{G^-}[d]	ϕ_t[e]	ϕ_{g^+}[f]	ϕ_{g^-}[f]
C_6H_6	180.1 ± 11.7	81.8 ± 13.5	−81.0 ± 13.2	180.1 ± 9.4	75.8 ± 14.2	−75.3 ± 14.4
H_2O		63.7 ± 9.4	−68.3 ± 9.4	−171.0 ± 8.0	98.5 ± 10.1	−97.4 ± 9.6

[a] The bond lengths in angstroms. [b] The bond angles in degrees. [c] The trans torsion angle around the C−C bond in degrees. [d] The gauche torsion angle around the C−C bond. [e] The trans torsion angle around the C−O bond. [f] The gauche torsion angle around the C−O bond.

from unperturbed chains to the melts.[7] They concluded that the population changes result from the intermolecular O···CH$_3$ interactions and give rise to an extension of the chain in the melt[8] relative to the unperturbed chain in Θ solutions.[9] The values of $p_{G^{\pm}t}^{CCO}$ and $p_{G^{\pm}g^{\mp}}^{CCO}$ obtained from our simulation in a benzene solution listed in Table 3 are very similar to those for the unperturbed POE chains obtained by Smith et al.,[7] also shown in the table. Since there is no intermolecular O···CH$_3$ interaction in the current POE-benzene system, our result seems to warrant Smith et al.'s rational for the cause of the extended POE chain in the melt. In an aqueous solution, on the other hand, $p_{G^{\pm}t}^{CCO}$ has the largest value among the systems listed in the table. This is a consequence of a helix in which the conformation of the C−O bond prefers either trans (t) or the same sign of gauche ($g^{\pm}$) as that of gauche ($G^{\pm}$) for the preceding C−C bond such as $G^{\pm}t$ or $G^{\pm}g^{\pm}$.

Table 4 lists the average geometrical values of POE over 5 ns of the simulation in a benzene solution and those obtained from the aqueous solution simulation.[5] The COC bond angle is more sensitive to the solvent due to its smaller bending force constant, 149 kcal mol^{-1}, than the CCO bending force constant, 172 kcal mol^{-1}. The average torsion angles in a benzene solution are closer to those previously predicted by MP2 ab initio geometry optimization of 1,2-DME in the gas phase, $\langle\phi_{G^{\pm}}\rangle = \pm 74.8°$ and $\langle\phi_{g^{\pm}}\rangle = \pm 77.4°$.[17] This suggests a relatively small solvent effect on the torsion angles in a benzene solution. Also, larger rms deviations in the torsion angles, compared to the aqueous solution, are consistent with the greater flexibility of the torsional fluctuation in a benzene solution. On the other hand, a considerable shift is observed on the average torsion angles in an aqueous solution. This is likely to be related to POE's helical conformation in water. Similar changes in the torsion angles were made by Depner et al.'s simulation.[12] These average geometrical parameters are difficult to obtain experimentally.

Before we close the section for the conformation of POE, it is of interest to examine the effect of the force field on the POE conformation in light of the solvent effect. We performed an additional simulation of POE in benzene solution for 5 ns in which the POE's *intra*molecular interactions were described by the previous force field for a POE-water system while all *inter*molecular interactions were treated by the current force field. The simulation procedure was the same as discribed above. This will shed light on two issues: is the helix observed in water a result of the *intra*molecular force field for the POE chain, and does the current *intra*molecular force field have any effect on the random coil in benzene solution? The result indicated that the POE chain still transformed from a helix to a random coil in benzene, which shows basically the same conformational characteristics as those for the random coil observed in benzene solution above: $\langle R^2\rangle^{1/2} = 15.01 \pm 6.12$ Å, $\langle S^2\rangle^{1/2} = 9.82 \pm 2.53$ Å, $p_{G^{\pm}} = 0.79$, and $p_{g^{\pm}} = 0.20$.[30] In comparison between the two solutions, the largest difference in the *inter*molecular interactions stems from the electrostatic interactions since the benzene molecules bear no charge. This observation suggests that the interactions leading to the alteration of the chain conformation are mainly *inter*molecular in nature, in particular, electrostatic. It was found in our previous study that the electrostatic interactions were dominated by the hydrogen bonds between POE and water molecules.[5] Next, we examine how the different chain conformation affects the chain dynamics of POE.

Local Chain Dynamics

In the following, we characterize the local chain dynamics of POE in a benzene solution and then discuss the difference in the chain dynamics from POE in water. Figure 7 shows typical trajectories of the torsion angles around the C−C and C−O bonds in a benzene solution. The actual numbers of the conformational transitions, several hundreds, are not depicted in Figure 7 due to the data used for the trajectories which were plotted only at every 5 ps. The inspection of the trajectories of the torsion angles for both C−C and C−O bonds indicated that during the 5 ns simulation, there was no direct conformational transition for G^+ (g^+) ↔ G^- (g^-) for which the transition only occurred via the T (t) conformation instead. This is due to the higher rotational barrier for the G^+ (g^+) ↔ G^- (g^-) transition, 8.43 (7.29) kcal mol^{-1}, than for the T (t) ↔ $G^{\pm}$ ($g^{\pm}$) transition, 2.45 (2.77) kcal mol^{-1} (see Table 2).

The conformational transition rate $k_{TG(tg)}$ for the C−C and C−O bonds averaged over all the bonds in the chain for 5 ns are listed in Table 5, along with those for the aqueous solution. They are defined as the number of transitions divided by the total simulation time.[12] A

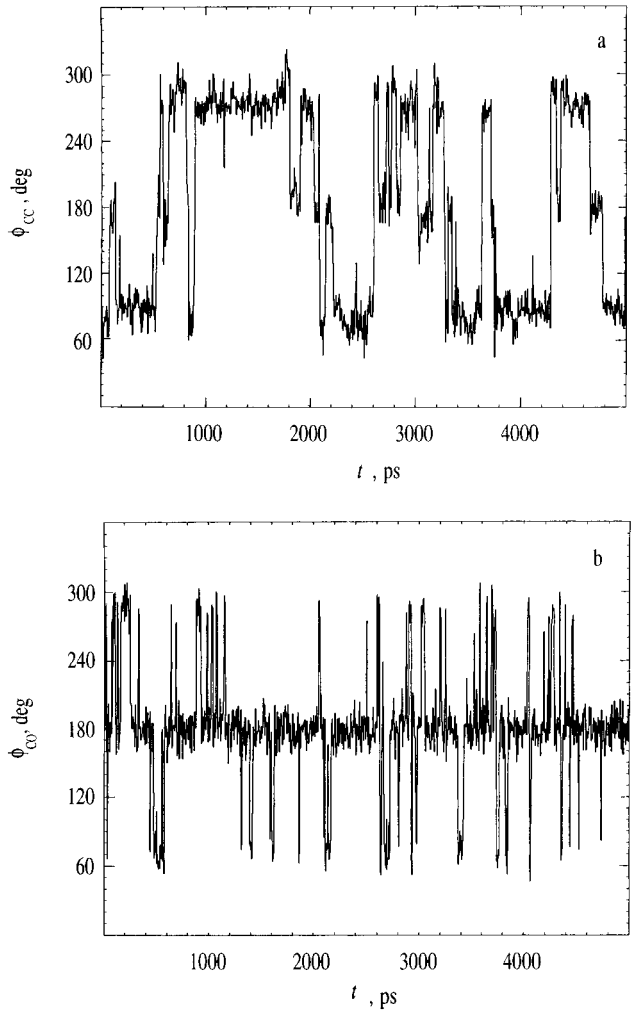

Figure 7. History of the torsion angles around (a) the C−C bond and (b) the C−O bond of POE obtained from the simulation in benzene. The data are plotted at every 5 ps.

Table 5. Conformational Transition Rates between Trans and Gauche Conformations $k_{TG(tg)}$ (ns^{-1}) and the Correlation Time τ (ps) for the Transition Process in Benzene and Water[a]

	C−C		C−O	
solvent	k_{TG}	τ	k_{tg}	τ
benzene	98.8	1.9	61	3.0
water	1.2[b]	0.0[b]	9.9	6.6

[a] See the definition for $k_{TG(tg)}$ and τ in the text. [b] The transitions occurred only for $G^+ \leftrightarrow T \leftrightarrow G^-$ with little residence time for the trans conformation.

significant difference is observed between the two solutions. In the aqueous solution, there were only a few conformational transitions for both C−C and C−O bond rotations during the 2 ns simulation. The value of k_{TG} is smaller than that for k_{tg} because the conformational transition for $T \leftrightarrow G^{\pm}$ in aqueous solution leads to a breakdown of a helix while a transition for $t \leftrightarrow g^{\pm}$ does not affect the stability of the helix as much. The much faster transition rates in the benzene solution indicate a smaller solvent damping in the bond rotations than in the aqueous solution.

According to Chandler,[31] the correlation time (τ) for the transition process can be estimated from the transition rates and the conformational populations, $n_{T(t)}$ and $n_{G(g)}$, as follows: $\tau = n_{T(t)}n_{G(g)}/k_{TG(tg)}$. The results are also shown in Table 5. In comparison, Depner and Schürmann reported 20 ps for both bonds.[12] However, the force field used in their simulations was not calibrated for POE. A higher rotational barrier around a bond can easily result in a large correlation time.

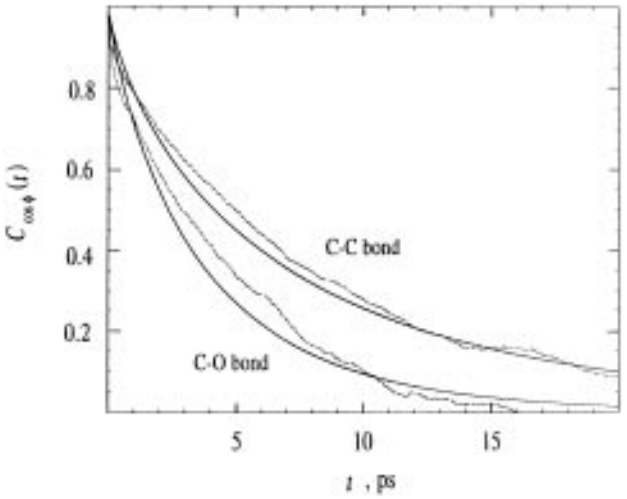

Figure 8. Torsion angle autocorrelation functions $C_{\cos\phi}(t)$ for the C−C and C−O bonds of POE in a benzene solution. The results were averaged over the chain except for the terminal group. The dotted lines are obtained from the trajectories taken from the simulation, and the solid curves are fits to the KWW equation.

Table 6. KWW Parameters for Torsion Angle Autocorrelation Functions[a]

bond	$\beta_{\cos\phi}$	$\tau_{\cos\phi}$, ps	τ_r, ps
C−C	0.77	6.71	7.77 ± 0.5
C−O	0.85	3.65	3.97 ± 0.5

[a] Averaged over all the internal bonds except the terminal bonds.

The relaxation time of the internal rotations of the chain can be estimated from the torsion angle (ϕ) autocorrelation function,[32]

$$C_{\cos\phi}(t) = \frac{\langle \cos\phi(t)\cos\phi(0)\rangle - \langle\cos\phi(0)\rangle^2}{\langle\cos\phi(0)\cos\phi(0)\rangle - \langle\cos\phi(0)\rangle^2} \qquad (2)$$

The averages were taken over the chain except for the terminal C−C or C−O bond since it has been found that the dynamics of the internal rotations near chain ends differ from that in the middle of the chain.[33] Figure 8 displays the decays of $C_{\cos\phi}(t)$ for the C−C and C−O bonds in benzene, shown by a dotted line, which are fitted to the Kohlraush−Williams−Watts (KWW) equation,[34] given as

$$C_{\cos\phi}{}^{\mathrm{KWW}}(t) = \exp(-t/\tau_{\cos\phi})^{\beta_{\cos\phi}} \qquad (3)$$

shown in the figure by a solid line. The relaxation time was calculated by the following equation:

$$\tau_r = \int_0^\infty \exp[-(t/\tau_{\cos\phi})^{\beta_{\cos\phi}}]\,\mathrm{d}t \qquad (4)$$

The KWW parameters obtained from least-squares fitting to the plots of $\ln[-\ln C_{\cos\phi}(t)]$ vs $\ln t$ and the relaxation time calculated from eq 4 are listed in Table 6.

The relaxation time τ_r for the C−O bond is almost half that for the C−C bond. This is in good accord with the experimental observation that the C−O bond rotation is more flexible than the C−C bond rotation,[2a,b] also consistent with the time evolution of the torsion angle

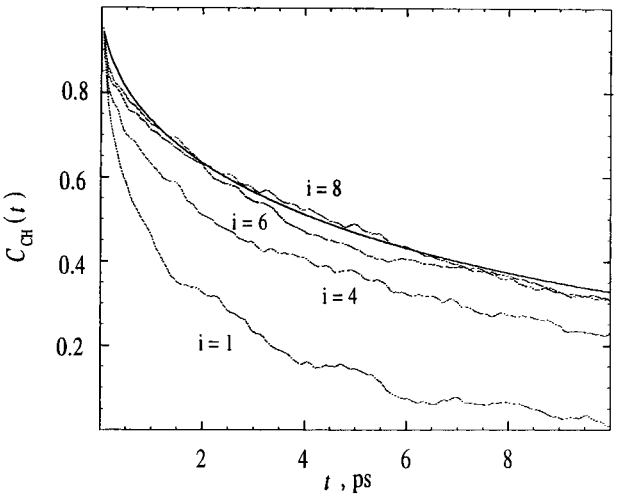

Figure 9. C−H vector autocorrelation functions $C_{CH}(t)$ for the carbon atoms from $i = 1$, 4, 6, and 8 in $CH_3O-[C_iH_2C_{i+1}H_2O]_{15}-CH_3$ in a benzene solution. A fit to the KWW equation is shown only for the carbon atom $i = 8$ at the center of the chain.

distribution for the C−O bond. On the other hand, a smaller value of $\beta_{\cos\phi}$ for the C−C bond than that for the C−O bond suggests a larger cooperativity for the C−C bond rotation. This is in line with the more correlated conformational rotations around the C−C−O bond pair than those around the C−O−C bond rotations due to the attractive 1−5 interaction for the C−C−O bond rotations.[18] This attractive interaction occurs in the $G^{\pm}g^{\mp}$ conformation which is one of the most stable conformations for the C−C−O bond pair of POE (see Table 2). In fact, the hazard plots showed more correlation for the C−C−O bond rotations than for the C−O−C bond rotations. The quantitative comparison with the aqueous solution simulation was not successful since there were very small changes in the value of cos $\phi(t)$ during the simulation in an aqueous solution, thus little decay in the torsion angle autocorrelation function.

We also examined the local segmental dynamics of POE by estimating the rate of the C−H vector reorientation. The C−H vector autocorrelation function was calculated by the following equation:[35]

$$C_{CH}(t) = \langle P_2(\mathbf{CH}(0)\cdot\mathbf{CH}(t))\rangle = \langle 3\cos^2\omega(t) - 1\rangle/2 \quad (5)$$

where P_2 is the second Legendre polynomial, $\mathbf{CH}(t)$ is a unit vector in the direction of a C−H bond vector at time t, and $\omega(t)$ is the change in the vector orientation between time t and time 0. Figure 9 shows the decays of $C_{CH}(t)$ for several C−H vectors ranging from the terminal CH_2 group ($i = 1$) to the central CH_2 group ($i = 8$) in $CH_3O-[C_iH_2C_{i+1}H_2O]_{15}-CH_3$, along with the fit of the decay for $i = 8$ to the KWW equation. The different local dynamics in going from the end to the center in the chain is well-illustrated. There was little difference in the C−H vector reorientation behavior between $i = 6$ and $i = 9$.

The values of the KWW parameters and the relaxation time are listed in Table 7 along with those for the POE aqueous solution. The agreement with the experiment[36] is reasonable. A substantial relative solvent effect is demonstrated. The large relaxation time, around 6 ns, for the aqueous solution is due primarily to the rigid helical chain, secondarily to the significant solvent damping, consistent with the extremely slow conformational transition rates in the aqueous solution.

Table 7. KWW Parameters for C−H Vector Autocorrelation Function[a]

solvent	β_{CH}	τ_{CH}, ps	τ_r, ps	τ_{exp}, ps[b]
C_6H_6	0.56	8.18	13.51 ± 1.1	15
H_2O[c]	0.3	1640	5790 ± 430	

[a] Averaged over the central CH vectors ($i = 6-9$) in $CH_3O-[C_iH_2C_{i+1}H_2O]_{15}-CH_3$. [b] Extrapolated from the value, 15.8 ps, measured at the concentration of 5 wt %[36] to 3.3 wt %, the solution concentration in our simulation. [c] Analyzed from the data in ref 5.

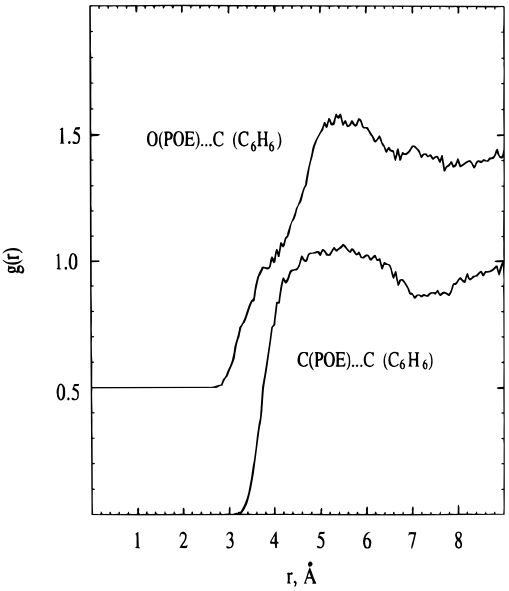

Figure 10. Pair distribution function for the POE ether oxygen atom and the nearby benzene carbon atoms ($O_{POE}\cdots C_{C_6H_6}$) and that for the POE methylene carbon atom and the nearby benzene carbon atoms ($C_{POE}\cdots C_{C_6H_6}$).

However, the values for the aqueous solution should be considered only qualitative.

Solvation Structure

Molecular dynamics simulations provide the information regarding solvation structures to help understand polymer−solvent interactions. Figure 10 illustrates a typical pair distribution function (PDF) for the POE ether oxygen atom and the nearby benzene carbon atoms and that for the POE methylene carbon atom and the nearby benzene carbon atoms. The POE oxygen−benzene carbon PDF (PDF($O_{POE}\cdots C_{C_6H_6}$)) displays a peak around 5.5 Å, while the POE methylene carbon−benzene carbon PDF (PDF($C_{POE}\cdots C_{C_6H_6}$)) shows a broad peak ranging from 4.0 to 6.5 Å with the center around 5 Å. Although the figure shows the PDF's for one of the benzene carbon atoms, the PDF's for other benzene carbon atoms exhibited very similar distribution profiles.[37] This observation suggests that the distances between the POE oxygen (or the methylene carbon) and all six benzene carbons are similar to each other.

We thus assume that an EO unit of POE orients itself perpendicular to the benzene molecular plane, rather than a horizontal orientation, shown in Figure 11. The numbers in the figure indicate the distances between the POE oxygen or the methylene carbon and the center of mass of a benzene molecule. The distance between the methylene carbon and the benzene's center of mass for all the models was taken to be 5 Å, based on the PDF ($C_{POE}\cdots C_{C_6H_6}$). Models I and II should yield the peak around 6 and 4 Å in the PDF ($O_{POE}\cdots C_{C_6H_6}$), respectively. On the other hand, the distance between

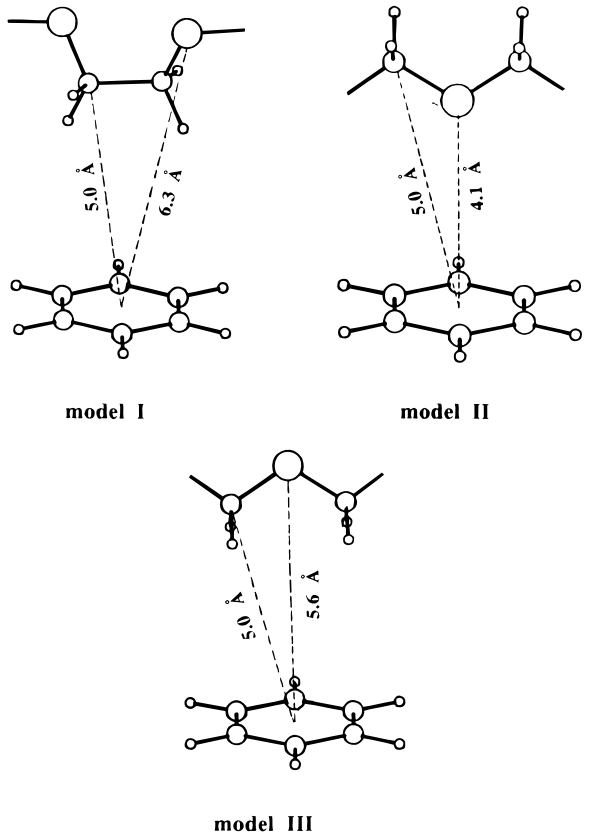

Figure 11. Proposed solvation models. The distances are between the POE oxygen or the methylene carbon and the center of mass of a benzene molecule.

O_{POE} and the benzene's center of mass, ~5.6 Å, in model III is close to the peak position in the PDF($O_{POE}\cdots C_{C_6H_6}$), ~5.5 Å, which favors model III as a most likely solvation structure for POE in a benzene solution, though our observation does not exclude models I and II due to the broad peak of the PDF($C_{POE}\cdots C_{C_6H_6}$). Also, the shoulder between 3 and 4 Å in the PDF ($O_{POE}\cdots C_{C_6H_6}$) seems to suggest some contribution from model II where the $O_{POE}\cdots C_{C_6H_6}$ distance is around 4 Å. The orientational preference of the benzene molecule with respect to the POE oxygen found in this sutdy is in agreement with Depner et al.'s study.[12]

An NMR high-field shift for the POE methylene proton in a benzene solution is well-known.[2b] A preferential orientation of the benzene molecule to the solute was excluded from a possible cause for a similar observation for poly(methyl methacrylate).[38] The orientation of the methylene protons with respect to the benzene ring illustrated in Figure 11, particularly models I and III, causing the aromatic ring current effect, is consistent with the experimental observation.[2b]

Figure 12 displays the PDF for the benzene carbons near the POE methylene carbon and the PDF for the bulk benzene carbons taken from the benzene simulation. The former shows similar characteristics to the latter. The peaks of the PDF for the benzene carbons near the POE methylene carbon seem to be somewhat flatter than those for the bulk benzene carbons, though it is not clear if this is statistically significant. No considerable difference between the two PDF suggests a very small perturbation of the solvent structure by POE, unlike the strongly enhanced water structure near POE observed in the previous simulation.[5] This observation implies little entropy loss for the benzene molecules near POE. This is in line with the observation

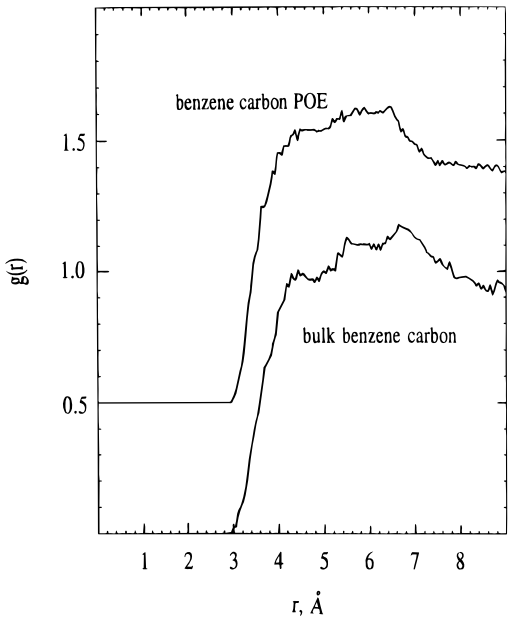

Figure 12. Pair distribution functions for the benzene carbon atoms near the POE methylene carbon atom and for the bulk benzene carbon atoms.

that POE does not precipitate in a benzene solution at elevated temperatures.[2d]

Conclusions

We have characterized the conformation and the dynamics of a POE chain with 15 monomer units in detail based on its 5 ns MD simulation in a benzene solution and compared them with the results from a previous simulation in aqueous solution. We observed significant differences in the POE characteristics in going from an aqueous solution to a benzene solution. Our main interest was how the difference in nature of the solvent affects the POE's characteristics. The absence of the hydrogen bond and the high polarity of water as a solvent has resulted in considerable changes in the conformation and the dynamics of POE. For example, in the simulation of POE in an aqueous solution, a helical conformation was maintained for 2 ns. In a benzene solution, the conformation quickly changed from a helix to a coil which continued to stay throughout the 5 ns simulation. This observation also supports the helical conformation found in the aqueous solution simulation[5] as a result of a solvation rather than an artifact. The population of the trans conformation around the C−C bond also increased considerably from 0 in water to 24% in benzene, and the conformational transition rates $k_{TG(tg)}$ jumped from 1.2 (9.9) in water to 98.8 (61.0) for the C−C (C−O) bond rotations in benzene. The sensitivity of the POE conformation to the solvent is largely due to its chain flexibility. The additional simulation in benzene solution with the intramolecular force field for the POE-water system also resulted in a random coil of POE. This observation confirms the significant alteration in the chain conformation as a result of the change in the POE-solvent interactions, the electrostatic interactions to be specific. In the POE aqueous solution, the intermolecular interactions were dominated by hydrogen bonds between POE and water molecules which are absent in the POE−benzene solution.

In an aqueous solution, POE seems to prefer a helix which is stabilized by a network of hydrogen bonds with

water which runs through inside the helix.[5] POE seems to gain a large negative enthalpy at a minimum cost to the entropy of water with the least disrupting structure to water, a helix. On the other hand, due to the absence of a hydrogen bond and the polarization effect, the helix is no longer stable in a benzene solution. The weak interactions between POE and benzene molecules, indicated by the much smaller POE-solvent interaction energy in benzene solution than in aqueous solution, result in a random coil which increases the configurational entropy of POE. Furthermore, the solvent structure near POE was less perturbed compared to the aqueous solution. The overall conformational characteristics are similar to those found by Depner et al.'s simulation.[12] Some discrepancies such as the somewhat higher gauche population around the C−C bond and the large correlation time for the conformational transitions found in their study are possibly due to the force field used and the short simulation time, 120 ps.

The absence of the hydrogen bond and the polarization effect also manifested themselves in the smaller solvent damping effect on the torsional rotations and the C−H vector reorientations of POE in benzene solution. On the other hand, in aqueous solution the ordered chain conformation and the much lower conformational transition rate and the large relaxation time for the C−H vector reorientations are due to the strong solvent effect giving rise to a rigid helical chain.

The pairwise populations, p_{Gt}^{CCO} and p_{Gg}^{CCO}, obtained from our simulation seem to support Smith et al.'s explanation[7] for an extended chain in POE melts, relative to the unperturbed chains. The NMR vicinal coupling constants[2j,11] are probably not very sensitive to the change in these particular pairwise populations. On the basis of the pairwise conformations, a POE chain seems to be less extended in benzene than in the melts, possibly closer to an unperturbed chain.

On the basis of the time evolutions of the conformational populations, the equilibrium characteristics of the POE chain do not seem to alter significantly after 5 ns. The information obtained from our POE simulation in benzene solution which either is difficult to probe experimentally or has not been previously reported includes the amplitudes and the fluctuations in R and S, the direct conformational populations including the pairwise populations, the average geometrical parameters, and the solvation structure.

We have also reoptimized the POE force field parameters, originally developed by Smith et al.[13] for the potential energy function commonly used in well-known molecular modeling packages such as QUANTA,[14] SYBYL,[15] AMBER,[39] and others. A comparison between the force field calculations with our parameters and the ab initio results of 1,2-DME[17,18] was favorable. The force field yielded good agreement with experiments in the conformational and the dynamical characteristics of POE in a benzene solution despite the fact that the force field was not specifically calibrated for a POE-benzene system. This observation supports the basic validity of Smith et al.'s force field[13] for a POE−benzene system. Together with the previous simulation,[5] simulations of a POE chain have been successfully performed in two solvent systems: water and benzene. This will open a possibility of performing a simulation for POE in a two-phase system, a POE−water/benzene system, which will be the subject of our forthcoming article.

Acknowledgment. The author greatly acknowledges the very helpful comments by Professor R. Yaris at Washington University, St. Louis. The computer time was made available by the Chemistry Computing Facility at Washington University.

References and Notes

(1) *Poly(Ethylene Glycol) Chemistry*; Harris, J. M., Ed.; Plenum: New York, 1992.
(2) (a) Liu, K.-J.; Parsons, J. L. *Macromolecules* **1969**, *2*, 529. (b) Liu, K.-J. *Macromolecules* **1968**, *1*, 213. (c) Liu, K.-J.; Ullman, R. *J. Chem. Phys.* **1968**, *48*, 1158. (d) Molyneux, P. *Water-Soluble Synthetic Polymers: Properties and Behavior*; CRC Press: Boca Raton, FL, 1983; Vol. 1, p 19. (e) Koenig, J. L.; Angood, A. C. *J. Polym. Sci.* **1970**, *8*, 1787. (f) Matsuura, H.; Fukuhara, K. *J. Mol. Struct.* **1985**, *126*, 251. (g) Allen, G.; Booth, C.; Hurst, S. J.; Jones, M. N. Prices, C. *Polymer* **1967**, *8*, 391. (h) Maxfield, J.; Shepherd, I. W. *Polymer*, **1975**, *16*, 505. (i) Bailey, F. E., Jr.; Koleske, J. V. *Poly(ethylene oxide)*; Academic Press: New York, 1976. (j) Tasaki, K.; Abe, A. *Polym. J.* **1985**, *17*, 641.
(3) (a) Zuniga, I.; Bahar, I.; Dodge, R.; Mattice, W. L. *J. Chem. Soc.* **1991**, *95*, 5348. (b) Theodorou, D.; Suter, U. W. *Macromolecules* **1986**, *19*, 1467. (c) Smith, G. D.; Jaffe, R. L.; Yoon, D. Y. *Ibid.* **1993**, *26*, 298. (d) Kremer, K.; Grest, G. S. *J. Chem. Soc.* **1990**, *92*, 5057. (e) McKechnie, J. L.; Haward, R., N.; Brown, D.; Clarke, J. H. R. *Macromolecules* **1993**, *26*, 198. (f) Pant, P. V. K.; Han, J.; Smith, G. D.; Boyd, R. H. *J. Chem. Phys.* **1993**, *99*, 597.
(4) (a) Depner, M.; Schürmann, B. L.; Auriemma, F. *Mol. Phys.* **1991**, *74*, 715. (b) Moe, N. E.; Ediger, M. D. *Macromolecules* **1995**, *28*, 2329. (c) Müller-Plathe, F. *Macromolecules* **1996**, *29*, 4782.
(5) Tasaki, K. *J. Am. Chem. Soc.* **1996**, *118*, 8459.
(6) Mark, J. E.; Flory, P. J. *J. Am. Chem. Soc.* **1966**, *88*, 3702.
(7) Smith, G. D.; Yoon, D. Y.; Jaffe, R. L.; Colby, R. H.; Krishnamoorti, R.; Fetters, L. J. *Macromolecules* **1996**, *29*, 3462.
(8) Kugler, J.; Fischer, E. W.; Peuscher, M.; Eisenbach, C. D. *Makromol. Chem.* **1983**, *184*, 2325.
(9) (a) Boucher, E. A.; Hines, P. M. *J. Polym. Sci., Polym. Phys. Ed.* **1978**, *16*, 501. (b) Ataman, M.; Boucher, E. A. *Ibid.* **1982**, *20*, 1585.
(10) Smith, G. D.; Jaffe, R.; Yoon, D. Y. *J. Am. Chem. Soc.* **1995**, *117*, 530.
(11) Abe, A.; Tasaki, K.; Mark, J. E. *Polym. J.* **1985**, *33*, 232.
(12) Depner, M.; Schürmann, B. L. *J. Comput. Chem.* **1992**, *33*, 1210.
(13) Smith, G. D.; Jaffe, R. L.; Yoon, D. Y. *J. Phys. Chem.* **1993**, *97*, 12752.
(14) Molecular Simulation, Inc., 9685 Scranton Road, San Diego, CA.
(15) Tripos Associate, Inc., 1699 S. Hanly Road, St. Louis, MO.
(16) Smith et al.'s force field[13] was developed primarily on the basis of gas-phase ab initio calculations.[18]
(17) Tasaki, K. *Polym. Prepr. (Am. Chem. Soc., Div. Polym. Chem.)* **1994**, *35*, 763.
(18) Jaffe, R. L.; Smith, G. D.; Yoon, D. Y. *J. Phys. Chem.* **1993**, *97*, 12745.
(19) (a) Karlström, G.; Linse, P.; Wallquist, A.; Jönsson, B. *J. Am. Chem. Soc.* **1983**, *105*, 3777. (b) Evans, D. J.; Watts, R. O. *Mol. Phys.* **1976**, *32*, 93. (c) Steinhauser, O. *Chem. Phys.* **1982**, *73*, 155. (d) Claessens, M.; Ferrario, M.; Ryckaert, J.-P. *Mol. Phys.* **1983**, *50*, 217.
(20) Jorgensen, W. L *J. Am. Chem. Soc.* **1981**, *103*, 335.
(21) The united atom approximation has been shown not to hamper correct descriptions of various liquids along with a rigid molecule model.[20]
(22) Narten, A. H. *J. Chem. Phys.* **1968**, *48*, 1630; **1977**, *67*, 2102.
(23) McCool, M. A.; Collings, A. F.; Woolf, L. A. *J. Chem. Soc., Faraday Trans. 1* **1972**, *68*, 1489.
(24) Tanaka, G.; Mattice, W. L. *Macromolecules* **1995**, *28*, 1049.
(25) An extrapolation from a viscosity measurement of POE in benzene solution yielded 20.8 Å for R_0.[2g]
(26) Theodorou, D. N.; Suter, U. W. *Macromolecules* **1985**, *18*, 1467.
(27) Tasaki, K.; McDonald, S.; Brady, J. W. *J. Comput. Chem.* **1993**, *14*, 278.
(28) The distance between the nearest POE oxygen atoms which is the same as the nearest O···O distance of water molecules, 2.80 Å, yields $\langle\phi_{G^\pm}\rangle_i = 68°$ when the bond lengths and the valence angles (the force field) listed in Table 2 were used.
(29) (a) Clarke, J. H. R. In *Computer Modelling of Fluids Polymers and Solids*; Catlow, C. R. A., Parker, S. C., Allen, M. P., Eds.; Kluwer Academic Publishers: Dordrecht, 1990; p 203. (b)

Edberg, R.; Evans, D. J.; Morris, G. P. *J. Chem. Phys.* **1986**, *84*, 6933. (c) Helfand, E. *Ibid.* **1978**, *69*, 1010.
(30) The increased gauche population around the C−C bond is due to the intramolecular force field used which was fitted to the observed higher gauche population of POE in water, compared to POE in nonpolar solutions.[2j] As a result, the molecular dimension decreased somewhat. On the other hand, the intramolecular force field for the POE−water system yields the rotational potential around the C−O bond which differs little from that calculated by the current intramolecular force field used for the POE− benzene solution.
(31) Chandler, D. *J. Chem. Phys.* **1978**, *68*, 2959.
(32) Takeuchi, H.; Roe, J. R. *J. Chem. Phys.* **1991**, *94*, 7446.
(33) Clarke, J. H. R.; Brown, D. *Mol. Phys.* **1986**, *58*, 815.
(34) Williams, G.; Watts, D. C. *Trans. Faraday Soc.* **1970**, *66*, 80.
(35) Moe, N. E.; Edger, M. D. *Macromolecules* **1995**, *28*, 2329.
(36) Heatley, F.; Walton, I. *Polymer* **1967**, *17*, 1020.
(37) Though all six benzene carbon atoms are chemically identical, individual carbon atoms can be distinguished by their atom numbers in the MD simulation.
(38) (a) Liu, K.-J. *J. Polym. Sci., Polym. Phys. Ed.* **1967**, *5*, 1199. (b) Liu, K.-J. *Ibid.* **1967**, *5*, 1209.
(39) Weiner, S. J.; Kollman, P. A.; Case, D. A.; Singh, U. C.; Ghio, C.; Alagona, G.; Profeta, S.; Weiner, P. *J. Am. Chem. Soc.* **1984**, *106*, 765.

MA9602785